Planar $\hat{l}$ textures and magnetic resonances in superfluid ^{3}He-A*

Kazumi Maki and Pradeep Kumar
Physics Department, University of Southern California, Los Angeles, California 90007
(Received 4 March 1977)

The three typical planar $\hat{l}$ textures in the presence of magnetic fields and currents are studied. Their texture profiles, energies, and associated magnetic resonance satellite frequencies are calculated. We propose that the splay $\hat{l}$ texture is responsible to the transverse satellite observed by Gould and Lee in their magnetic resonance experiment.

I. INTRODUCTION

The spin triplet, P-wave condensate of superfluid ^{3}He-A is characterized in terms of two unit vectors; $\hat{l}$ describes the symmetry axis along which the energy gap is zero, while $\hat{d}$ describes the direction of the linear spin momentum[1] of the condensate. These two vector fields are influenced by a variety of constraints[2]: (a) the dipole energy favors that $\hat{l}$ parallel or antiparallel to $\hat{d}$; (b) $\hat{l}$ has to be normal to the surface of the wall; (c) a current flow tends to orient $\hat{l}$ parallel to itself; and (d) $\hat{d}$ has to be perpendicular to a static magnetic field. The combined effect of these constraints gives rise to a particular arrangement of $\hat{l}$ and $\hat{d}$ fields referred to as textures.[3]

The simplest texture (theoretically, but not experimentally) is of course the uniform texture where $\hat{l}$ and $\hat{d}$, parallel to each other, are pointed in the same direction over the entire sample. However, this structure is *a priori* impossible in a cylindrical or a spherical container.[4,5] It becomes imperative therefore to study textures obtained by bending of $\hat{l}$ or $\hat{d}$ vectors. There are obtained as the local minima of a free energy that includes the contributions due to the bending of these vectors and various symmetry breaking terms mentioned above. Of the various nontrivial textures possible, the simplest are the planar textures or domain walls. These are the boundaries between two distinct equilibrium configurations of the ground state.

It is possible to classify the planar structures in ^{3}He-A as (i) pure $\hat{d}$ ($\hat{l}$ uniform); (ii) pure $\hat{l}$ ($\hat{d}$ uniform); (iii) composite. The first case, where $\hat{l}$ is fixed either due to walls or flow, has been studied[6,7] in some detail previously. These $\hat{d}$ structures, which we call $\hat{d}$ solitons, can be created magnetically.[7] A moving $\hat{d}$ solution carries a magnetization pulse, whose dynamics is described by a sine-Gordon equation. For example, the zero-energy mode associated with translational motion of $\hat{d}$ soliton appears as an unshifted satellite frequency in a nuclear magnetic resonance.[7]

In the third case of the composite structure, which we call composite soliton,[8] is found to be the minimum of free energy when both $\hat{l}$ and $\hat{d}$ are allowed to move. Indeed, if the surface pinning, which keeps $\hat{l}$ uniform, is not too strong, the twistlike $\hat{d}$ soliton is unstable towards the formation of a twist composite soliton. A characteristic feature of these textures is the coherent response in a nuclear-magnetic-resonance experiment. In a uniform system, the motion of $\hat{d}$ vector away from the $\hat{l}$ vector produces a constant torque responsible for the usual Leggett shifts.[2] In a nonuniform system, there exists a coherent motion of $\hat{d}$ vector, which gives rise to satellite resonances with lower frequencies than the main resonance with the Leggett shift. Furthermore, the intrinsic spatial inhomogeneity contributes an additional linewidth via the spin-diffusion effects. Recently we have shown that the composite soliton gives rise to satellite frequencies both in the longitudinal and the transverse magnetic resonance. In particular, the predicted longitudinal satellite frequency appears to account for the satellites found in the longitudinal magnetic resonance experiments by the Orsay-Saclay group[9] and more recently by Gould and Lee.[10] On the other hand, the predicted transverse satellite frequency was a little too high compared with the observed satellite by Gould and Lee[10] in their transverse experiment.

In this paper, we will study planar pure $\hat{l}$ textures in detail. In Sec. II, we obtain three typical planer textures: splay, bending, and twist textures by minimizing the free energy. Here the terms splay and bending are used in somewhat loose sense than are used in liquid crystals,[11] since we cannot have pure splay or pure bending planar structure. We limit ourselves to the case where a static magnetic field is applied in the z direction and a current flows in the y direction for simplicity. In this case three possible configurations mentioned above are shown in Fig. 1. The static magnetic field fixes equilibrium $\hat{d}$ and $\hat{l}$ vectors within the x-y plane, while the current determines $\hat{l}$ vector asymptotically (i.e., far from tex-

tures) in the y direction. In the present analysis the equilibrium $\hat{d}$ vector is assumed uniform and in the y direction. We have calculated analytic profiles for $\hat{l}$ vectors, the texture energies and associated satellite frequencies in nuclear magnetic resonance in Sec. III.

As opposed to a pure-$\hat{d}$ structure, where the splay soliton is of lowest energy, the twist structure is found to be the lowest-energy structure for pure-$\hat{l}$ case. However, the twist $\hat{l}$ structure is locally unstable toward the formation of the composite soliton, unless the flow is rather strong. On the other hand, the splay $\hat{l}$ texture appears as a natural product, if the static magnetic field is rotated by 90° from parallel to perpendicular direction to the cylindrical axis (and if twist composite solitons are in the cylinder in the beginning). Owing to the uniform current along the axis of the cylinder, the splay $\hat{l}$ textures appear to be stabilized in spite of their higher energy than the twist $\hat{l}$ textures. Furthermore, the calculated transverse satellite frequency associated with the splay $\hat{l}$ texture agrees beautifully with the observed satellite in their transverse experiment by Gould and Lee.[10] Therefore we believe that in the Gould-Lee experiment, two completely different textures are involved. The longitudinal satellites are due to the composite solitons as already proposed, while the transverse satellites are due to the splay $\hat{l}$ textures. The present identification may be easily verified, if a similar experiment is done with a rf field perpendicular to the cylindrical axis. In this geometry we expect that one will see the longitudinal satellite associated with the splay $\hat{l}$ texture and the transverse satellite associated with the composite soliton.

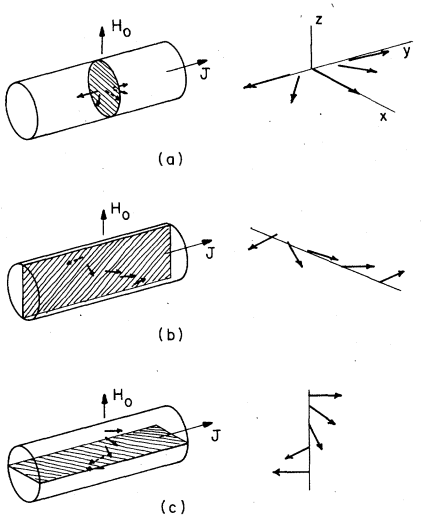

FIG. 1. Various planar textures studied in this paper: (a) splay; (b) bending; and (c) twist. The arrow indicates the direction of $\hat{l}$ vector. The $\hat{d}$ vector is uniformly in the y direction.

II. TEXTURE PROPERTIES

In the superfluid ^{3}He-A, the nine-component complex order parameter is given by $A_{i\alpha}=\Delta_i\hat{d}_\alpha$, where

$$\Delta_i=(\Delta_0/\sqrt{2})(\hat{\delta}_1+i\hat{\delta}_2)_i\,. \tag{1}$$

Here Δ_0 is the amplitude of the order parameter; $\hat{\delta}_1$, $\hat{\delta}_2$, and $\hat{l}$ ($\equiv\hat{\delta}_1\times\hat{\delta}_2$) constitute the orthogonal triad of unit vectors in real space; and $\hat{d}$ is a unit vector describing the spin configuration. The free energy $F_{\rm kin}$ associated with the spatial variation of the order parameter has been derived by Ambegaokar *et al.*[12]:

$$F_{\rm kin}=\tfrac{1}{2}\int d^3r\,[K_1\partial_i A_{i\alpha}\partial_j A^*_{j\alpha}+K_2\partial_i A_{j\alpha}\partial_i A^*_{j\alpha} +K_3\partial_i A_{j\alpha}\partial_j A^*_{i\alpha}]\,. \tag{2}$$

In the Ginzburg-Landau regime (T near T_c), and with the assumption of the weak coupling (where $K_1=K_2=K_3=K$), we have

$$F_{\rm kin}=\tfrac{1}{2}K\int d^3r\,[3|\vec{\nabla}\cdot\vec{\Delta}|^2+|\vec{\nabla}\times\vec{\Delta}|^2+2|(\vec{\Delta}\cdot\vec{\nabla})\hat{d}|^2 +|\vec{\Delta}|^2(|\vec{\nabla}\cdot\hat{d}|^2+|\vec{\nabla}\times\hat{d}|^2)] \tag{3}$$

and

$$K=\tfrac{6}{5}(N/8m^*)7\zeta(3)/(2\pi T_c)^2\,,$$

with N being the density of ^{3}He atoms and m^* the effective mass of the quasiparticles. There are pure divergence terms associated with $F_{\rm kin}$ but for our calculations, they cancel themselves to zero. In order to discuss textures $F_{\rm kin}$ has to be supplemented by the nuclear dipole energy which takes the form[2]

$$E_D=-\tfrac{1}{2}\chi_N\Omega_A^2(\hat{l}\cdot\hat{d})^2\,, \tag{4}$$

where χ_N is the normal static spin susceptibility and Ω_A is the A phase longitudinal resonance frequency. To include the effect of the strong magnetic field $\vec{H}_0\|\hat{z}$, we assume that $\hat{d}=\hat{y}$ and

$$\hat{l}=\sin\chi\hat{x}+\cos\chi\hat{y}\,, \tag{5}$$

where χ is a function of space. The vector order parameter $\vec{\Delta}$, consistent with Eq. (5), is then given by

$$\vec{\Delta}=(\Delta_0/\sqrt{2})e^{i\Phi}(-\cos\chi\hat{x}+\sin\chi\hat{y}+i\hat{z})\,, \tag{6}$$

with Φ to be specified later. To obtain the texture profile, we substitute Eq. (6) into Eq. (3) and then minimize Eq. (3) with respect to χ. A general planar solution can be obtained by assuming $\chi=\chi(s)$ and $\Phi=\Phi(s)$, with $s=\hat{k}\cdot\vec{r}$, where $\hat{k}$ is a unit

vector normal to the domain wall thus obtained. An intrinsic phase current of the form $\hat{k}\partial\Phi/\partial s$ is obtained. However, this intrinsic current disappears if the spatial inhomogeneity is along one of axes of our coordinate system. In the presence of an external current, Φ takes a form $\Phi = qy$ in our geometry, where q is related to the velocity of Cooper pairs carrying the supercurrent by $q = 2Mv_s$, just as in the case of superconductor. It is true, in general, that the total current is expressed as the sum of the three components; $\nabla\Phi$, Mermin-Ho term due to spatial change of $\hat{l}$,[4] and curl $\hat{l}$. However, for the planar texture discussed here the second contribution vanishes identically. Furthermore curl $\hat{l}$ does not contribute to the total current in the y direction. Therefore we may simply assume that q is proportional to the superflow in the y direction. The inclusion of a flow term by $\Phi = qy$, gives rise to, in Eq. (3), an additional energy, which favors alignment of $\hat{l}$ vector in the y direction. Therefore, in the following we will concentrate on pure $\hat{l}$ asymptotically parallel to the y axis [i.e., $\chi(\infty), \chi(-\infty) = 0, \pi, \ldots$].

In the following we limit ourselves to three typical pure $\hat{l}$ textures.

A. $\hat{k} = \hat{x}$ (bending)

Substituting Eq. (6) with $\Phi = qy$ and $\chi = \chi(x)$ into Eq. (3), we have

$$\frac{F}{\sigma_x} = \tfrac{1}{2}A\int_{-\infty}^{\infty} dx\,[(1+2\sin^2\chi)\chi_x^2 + 2q^2\sin^2\chi + 4\xi^{-2}\sin^2\chi], \tag{7}$$

where $A = \frac{1}{2}K\Delta_0^2 = \frac{1}{4}\chi_N C_\perp^2$, $C_\perp$ being the spin-wave velocity, $\xi = C_\perp/\Omega_A$ the dipolar coherence length, and the subscript on χ represents derivative with respect to x. We note that in pure $\hat{l}$ texture the current adds a term proportional to $q^2\sin^2\chi$, while the last term in Eq. (7) arises from the dipolar energy.

After minimization with respect to χ, the texture profile and the corresponding energy are obtained as

$$\frac{x}{\xi} = \frac{1}{\sqrt{2}}(\phi - \tfrac{1}{2}\pi) - \tfrac{1}{4}\ln\left(\frac{\sqrt{2}\tan\phi + 1}{\sqrt{2}\tan\phi - 1}\right),$$

$$\cos\phi = \sqrt{\tfrac{2}{3}}\cos\chi, \tag{8}$$

and

$$F/\sigma_x = 2[1 + (3/\sqrt{2})\sin^{-1}\sqrt{\tfrac{2}{3}}\,]A\xi^{-1} \cong 0.756\, f^{\hat{d}}, \tag{9}$$

where $f^{\hat{d}} = 8A\xi^{-1}$ is the surface energy of pure (twist) $\hat{d}$ soliton.[7] We shall use $f^{\hat{d}}$ for reference. In the above treatment we have neglected q-dependent terms, since the effect of the q^2 term is easily included by replacing $4\xi^{-2}$ by $4\xi^{-2} + 2q^2$.

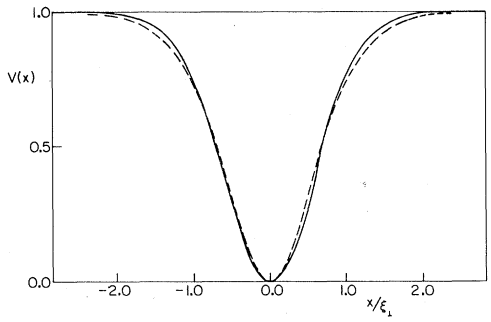

FIG. 2. Potential $V(x) = \cos^2\chi$ for the bending texture. The solid line represents the exact potential, while the dashed line represents the variational approximation. The latter is used for the calculation of satellite frequencies.

Equation (8) is rather difficult to invert for the solution of $\chi(x)$. Since it is necessary to know $\chi(x)$ in order to study the NMR frequency, we have tried a simple variational solution to Eq. (7) in a form $\cos\chi = \tanh(\eta x)$ with η being the variational parameter. In Fig. 2, we have plotted $\cos^2\chi$ [referred to as $V(x)$ since $\cos^2\chi$ is the potential in NMR frequency calculation] as obtained from Eq. (8) as well as the variational solution with $\eta = 2\sqrt{\frac{3}{7}}\,\xi^{-1}$. The agreement is rather encouraging. The energy for the variational approximation is found to be

$$F_v/\sigma_x = 0.764\, f^{\hat{d}}, \tag{10}$$

which is very close to the exact result of Eq. (9).

B. $\hat{k} = \hat{y}$ (splay)

For this case, assuming that $\chi = \chi(y)$, we have

$$\frac{F}{\sigma_y} = \tfrac{1}{2}A\int_{-\infty}^{\infty} dy\,[(1+2\cos^2\chi)\chi_y^2 + 4\xi^{-2}\sin^2\chi]. \tag{11}$$

The q-dependent term can be easily included as before by replacing ξ^{-2} by $\xi^{-2} + \frac{1}{2}q^2$. The texture profile and the energy are given by

$$\frac{y}{\xi} = \frac{1}{\sqrt{2}}\theta - \tfrac{1}{4}\sqrt{3}\ln\left(\frac{1+\sqrt{\frac{3}{2}}\tanh\theta}{1-\sqrt{\frac{3}{2}}\tanh\theta}\right), \tag{12}$$

with

$$\cos\chi = (1/\sqrt{2})\sinh\theta$$

and

$$F/\sigma_y = 2[\sqrt{3} + (1/\sqrt{2})\ln(\sqrt{2}+\sqrt{3})]A\xi^{-1} \simeq 0.6356\, f^{\hat{d}} \tag{13}$$

The energy is smaller than the bending texture energy. Again a variational approximation of the form $\cos\chi = \tanh(\zeta y)$ is tried. The comparison between exact $\cos^2\chi$ and variational one is shown in Fig. 3. The energy is minimized for $\zeta = 2\sqrt{\frac{3}{5}}\,\xi^{-1}$,

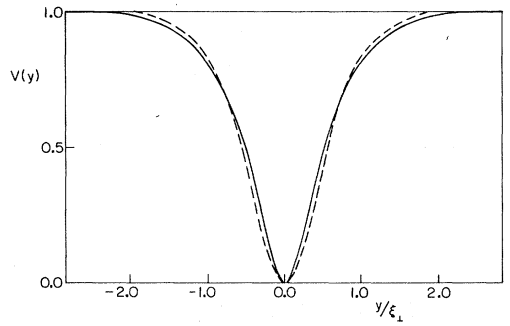

FIG. 3. Potential $V(y)=\cos^2\chi$ for the splay structure. Solid line, exact solution; dashed line, variational approximation.

with

$$F_v/\sigma_y = 0.645\ f^{\hat{d}}\ . \tag{14}$$

C. $\hat{k}=\hat{z}$ (pure twist)

For this case, Eq. (3) reduces to

$$\frac{F}{\sigma_z} = \tfrac{1}{2}A\int_{-\infty}^{\infty} dz\ (\chi_z^2 + 4\xi^{-2}\sin^2\chi)\ . \tag{15}$$

The analytical solution of Eq. (15) is given by

$$\chi = 2\tan^{-1}[\exp(2z/\xi)] \tag{16}$$

and

$$F/\sigma_z = 4A\xi^{-1} = 0.5\ f^{\hat{d}}\ . \tag{17}$$

As noted earlier in the Introduction, the energy of pure twist domain wall is the lowest. (See also Fig. 4.)

III. MAGNETIC RESONANCE

As the $\hat{d}$ vector moves away from the $\hat{l}$ vector, it experiences the dipolar torque. In nuclear magnetic resonance this dipolar torque provides the Leggett shifts in the resonance frequencies. In a nonuniform texture like a domain wall considered here, there are regions where the effective potential energy for $\hat{d}$ vector oscillations is weaker. The result is that for textures, a normal mode of oscillations exists that is localized at the domain wall and the characteristic frequency is less than the usual Leggett shifted resonance frequency. Such effects then should be observable in a magnetic resonance experiment. The relation between the NMR frequencies and the eigenvalues associated with the $\hat{d}$ vector fluctuations has been described in a previous paper.[8] In this paper we present the eigenvalue calculation of $\hat{d}$ fluctuations in pure $\hat{l}$ textures.

Assuming that $\hat{d}$ is now given by

$$\hat{d} = f\hat{x} + (1-f^2-g^2)^{1/2}\hat{y} + g\hat{z}\ , \tag{18}$$

where f and g are space-dependent functions, we can expand the spin part of the free energy up to terms of order f^2 and g^2. The diagonalization of the second-order term, referred to as fluctuation free energy, yields the NMR frequencies. Although, in general, a term linear in f appears in the free energy, this term can be eliminated by modifying the equilibrium configuration slightly since the quadratic term is positive definite. In any case, the presence of the linear term does not affect the response frequency of $\hat{d}$ vector. In the following we will discuss the NMR frequencies for three configurations separately.

A. Bending

The fluctuation free energy due to $\hat{d}$ fluctuations is given by

$$\frac{\delta F}{\sigma_x} = \tfrac{1}{2}A\int_{-\infty}^{\infty} dx\ [f\Lambda_f f + g\Lambda_g g]\ , \tag{19}$$

where

$$\Lambda_f f = -2\partial_x[(1+\cos^2\chi)f_x] + 4\xi^{-2}(\cos^2\chi - \sin^2\chi)f \tag{20}$$

and

$$\Lambda_g g = -2\partial_x[(1+\cos^2\chi)g_x] + 4\xi^{-2}\cos^2\chi g\ . \tag{21}$$

The eigenvalue equations are given by

$$\lambda f = \tfrac{1}{4}\xi^2\Lambda_f f \quad\text{and}\quad \lambda g = \tfrac{1}{4}\xi^2\Lambda_g g\ , \tag{22}$$

respectively. The above equations have one bound state each, which gives rise to satellite resonance in the NMR experiment. The satellite frequencies are given in terms of the eigenvalues λ_f and λ_g as

$$\omega_l/\Omega_A = (\lambda_f)^{1/2} \quad\text{and}\quad (\omega_l^2-\omega_0^2)^{1/2}/\Omega_A = (\lambda_g)^{1/2}\ , \tag{23}$$

respectively, for the longitudinal and the transverse satellite, respectively, where $\omega_0=\gamma_0 H$ is the Larmor frequency. In order to solve Eq. (22),

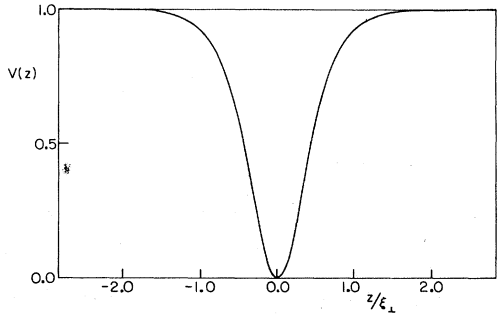

FIG. 4. Potential $V(z)=\cos^2\chi$ for the twist solution.

first, we approximate $\cos\chi$ by a variational solution, $\cos\chi = \tanh(\eta x)$ with $\eta = 2\sqrt{\frac{3}{7}}\,\xi^{-1}$. The resultant potential for the transverse mode $V(x) \propto \cos^2\chi$ is shown in Fig. 2, together with the exact result for comparison. Second, we determine the eigenvalue variationally by assuming that

$$f \propto [\mathrm{sech}(\eta x)]^{\nu}, \quad g \propto [\mathrm{sech}(\eta x)]^{\mu}, \tag{24}$$

with ν and μ being the variational parameters. The results are

$$\lambda_f = 0.1165, \quad \nu = 0.855, \quad \lambda_g = 0.6873, \quad \mu = 0.48, \tag{25}$$

implying

$$\omega_l/\Omega_A = 0.3413, \quad (\omega_t^2 - \omega_0^2)^{1/2}/\Omega_A = 0.829 \tag{26}$$

for longitudinal and transverse satellite frequencies.

Comparing the potential $V(x)$ for the $\hat{l}$ texture to that of $\hat{d}$ soliton, the potential has the same depth but the width is roughly $\frac{1}{2}$ smaller. Therefore we can conclude that the above are the only bound states associated with $\hat{l}$ texture.

B. Splay

The corresponding operators Λ_f and Λ_g are now given by

$$\Lambda_f f = -2\partial_y[(1+\sin^2\chi) f_y] + 4\xi^{-2}(\cos^2\chi - \sin^2\chi) f, \tag{27}$$

$$\Lambda_g g = -2\partial_y[(1+\sin^2\chi) g_y] + 4\xi^{-2}\cos^2\chi g, \tag{28}$$

respectively. Again we have used a variational form for χ in order to solve the eigenvalue problem. The variational potential $\cos^2\chi$ is plotted in Fig. 3 for comparison with the exact potential.

The eigenvalue equation (22) with new Λ_f and Λ_g given in Eqs. (27) and (28) is solved variationally by assuming that

$$f \propto [\mathrm{sech}(\zeta y)]^{\nu}, \quad g \propto [\mathrm{sech}(\zeta y)]^{\mu}. \tag{29}$$

We find now

$$\lambda_f = 0.1559, \quad \nu = 0.675, \quad \lambda_g = 0.6835, \quad \mu = 0.435, \tag{30}$$

respectively.

The corresponding satellite frequencies are now given by

$$\omega_l = 0.3948\,\Omega_A, \quad (\omega_t^2 - \omega_0^2)^{1/2} = 0.8267\,\Omega_A, \tag{31}$$

for longitudinal and transverse resonance, respectively.

These numbers are of particular interest in view of the recent observations of Gould and Lee.[8] They observed satellite resonances in NMR experiments with relatively open geometry. Their longitudinal satellite appeared at $0.74\,\Omega_A$ (with a weak temperature dependence) and the transverse satellite appeared at $(\omega_t^2 - \omega_0^2)^{1/2} = 0.83\,\Omega_A$ (with no discernible temperature dependence). There was however a crucial difference between the two experiments. For longitudinal resonance the static as well as the rf fields were axial to a cylinder, while in the transverse experiment, the rf field is axial but the static field was rotated to be perpendicular to the cylinder axis.

The value of longitudinal resonance frequency agrees very well with the predicted frequency in the presence of composite solitons[6] ($\omega_l \simeq 0.73\,\Omega_A$). We propose here that the transverse satellite originates from the pure $\hat{l}$ splay texture. Not only the $\hat{l}$ texture accounts for the transverse satellite frequency [compare Eq. (31) with the observed value $0.83\,\Omega_A$] but also we can show that in the case of a cylinder, if we start with pure twist composite solitons in the longitudinal geometry as described above, and if the static magnetic field is rotated by 90°, splay $\hat{l}$ textures are the end products.

For this purpose, we note that we need three vectors to characterize experimental situation; $\vec{H}_0$; asymptotic direction of $\hat{l}$, and $\hat{k}$ the normal vector of the domain wall. Furthermore, $\hat{l} \perp \vec{H}_0$ always since $\hat{d} \perp \vec{H}_0$ in the equilibrium configuration. In the longitudinal geometry in a cylinder, where $\vec{H}_0$ is parallel to the cylindrical axis, the composite solitons with $\hat{k} \parallel \vec{H}_0$ is the most stable configuration; $\hat{k}$ is parallel to the cylindrical axis. If we assume that the spatial inhomogeneity is locked in the cylinder, this implies $\hat{k}$ is always parallel to the axis. Then if we rotate $\vec{H}_0$ in the direction perpendicular to the axis, $\hat{l}$ rotates accordingly. In the presence of a flow along the axis of cylinder, $\hat{l}$ becomes parallel to the axis in the transverse geometry. In this situation $\hat{k} \parallel \hat{l}$, implying the splay texture. It is possible to test the present identification experimentally. If the rf field is applied perpendicular to the cylindrical axis, assignment of textures for longitudinal and transverse experiments is reversed. In this experiment, the satellite frequencies should be

$$\omega_l/\Omega_A = 0.3948, \quad (\omega_t^2 - \omega_0^2)^{1/2}/\Omega_A = 0.8944$$

if our identification is correct.

C. Twist

In this case we have

$$\Lambda_f f = -4f_{zz} + 4\xi^{-2}(\cos^2\chi - \sin^2\chi) f, \tag{32}$$

$$\Lambda_g g = -4g_{zz} + 4\xi^{-2}\cos^2\chi g, \tag{33}$$

where $\cos\chi = \tanh(2z/\xi)$.

The corresponding eigenvalue equations are exactly solved with

$$\lambda_f = 2\sqrt{3} - 2 = 0.4641\,, \qquad f = [\mathrm{sech}(2z/\xi)]^{(\sqrt{3}-1)/2} \tag{34}$$

and

$$\lambda_g = 2(\sqrt{2} - 1) = 0.828\,, \qquad g = [\mathrm{sech}(2z/\xi)]^{(\sqrt{2}-1)/2}\,, \tag{35}$$

implying

$$\omega_l/\Omega_A = 0.6812, \quad (\omega_t^2 - \omega_0^2)^{1/2}/\Omega_A = 0.9102\,. \tag{36}$$

However, as we will show in the appendix, the twist $\hat{l}$ texture is unstable toward formation of the composite soliton, unless current is rather large. Therefore, this last solution may be of little relevance to reality.

IV. CONCLUSION

We have studied three possible configurations (textures) of the spatially inhomogeneous $\hat{l}$ vector with the d vector held uniform over the entire sample. The three textures can be described in terms of relative orientation of three axes: the direction of spatial inhomogeneity $\hat{k}$ (direction normal to the domain wall surface); the static magnetic field $\vec{H}_0$; and the current flow direction that determines the equilibrium direction of the $\hat{l}$ vector $\vec{J}$. Furthermore, we limit ourselves to the case $\vec{H}_0 \perp \vec{J}$. The three textures are then: $\hat{k} \| \vec{J}$ (splay), $\hat{k} \| \vec{J} \times \vec{H}_0$ (bending), and $\hat{k} \| \vec{H}_0$ (twist). Energy calculations indicate $f_{\text{bend}} > f_{\text{splay}} > f_{\text{twist}}$. Analytical profiles for each texture have been obtained as the minima of the free energy.

Perhaps the most interesting result appears in the calculation of nuclear-magnetic-resonance frequencies. Each texture is found to have characteristic satellite frequencies, lower than the usual Leggett shift in the uniform case. In particular, the transverse satellite appearing in splay structure has a frequency identical to the one observed recently by Gould and Lee. In the Introduction as well as in Sec. III, we have presented arguments as to how a splay structure could be found in their experiment. However, it has to be borne in mind that at the time of writing, we cannot eliminate the possibility that they may be due to the splay composite soliton rather than pure $\hat{l}$ textures. We expect that the splay composite soliton has almost identical satellite frequencies as the splay $\hat{l}$ texture discussed here.

The characteristic satellite frequencies for known planar textures ($\hat{d}$ soliton, composite soliton) are summarized in Table I, together with the result of the present analysis for $\hat{l}$ textures. In the table, R_l and R_t are the normalized resonance shifts defined by $R_l = \omega_l/\Omega_A$ and $R_t = (\omega_t^2 - \omega_0^2)^{1/2}/\Omega_A$, with ω_l and ω_t being the transverse satellite frequencies. We include in the table the half width of resonances, which is given by $\Gamma = \frac{1}{2}D\langle|\vec{\nabla} f|^2\rangle$, with D the spin-diffusion constant, since the spin-diffusion term dominates the relaxation at least in the vicinity of T_c. Here f is the normalized bound-state wave function associated with the satellite and the angular bracket means the integral all over space. In more general situation, D has to be replaced by an appropriate component of the spin-diffusion tensor in superfluid ^{3}He-A. Substituting D measured by Wheatley[13] (extrapolated to $T = T_c$) and $\xi = 1.85\times10^{-3}$ cm, we have $D\xi^{-2} = 8.8\times10^3$ sec^{-1}. Then this gives the half width $(\Delta\omega_l)$ for the longitudinal satellite associated with the composite soliton $(\Delta\omega_l) \cong 1.3\times10^3$ Hz, which is compared with the one deduced from the Gould-Lee experiment $(\Delta\omega_l) \simeq 4.5\times10^3$ Hz. The predicted width is roughly a factor of 3 smaller than the one observed. However, taking into account ambiguities in extracting $\Delta\omega_l$ from the experimental data, we may conclude that the spin diffusion accounts for most of the

TABLE I. Summary of characteristic satellite frequencies for known planar textures.

		$f/(8A\xi^{-1})$	R_l	R_t	$\Delta\omega_l/(D\xi^{-2})$	$\Delta\omega_t/(D\xi^{-2})$
$\hat{d}$ soliton	Splay	$1/\sqrt{2}$			$\frac{1}{3}$	$\frac{1}{3}$
	Bending	1	0	0	$\frac{1}{6}$	$\frac{1}{6}$
	Twist	1			$\frac{1}{6}$	$\frac{1}{6}$
$\hat{l}$ texture	Splay	0.635	0.395	0.826	0.46	0.20
	Bending	0.757	0.341	0.829	0.23	0.12
	Twist	0.5	0.68	0.901	0.15	0.06
Composite	Splay					
Soliton	Bending			?		
	Twist	$1/\sqrt{5}$	0.722	0.894	0.145	0.07

width observed.

We note that the planar $\hat{l}$ structure may also be realized at the wall of the container, if a static magnetic field is applied normal to the wall. In this case a bending $\hat{l}$ texture with $\hat{k}$ parallel to the static field appears pinned at the wall, if the static field is sufficiently strong. In this case, we expect that the satellite resonance as calculated for the bending texture appears. However, since in the present geometry the static field lies in the plane where $\hat{l}$ and $\hat{d}$ are confined, assignment of the longitudinal and the transverse frequencies has to be interchanged; in the present geometry the expected satellite frequencies are $\omega_l/\Omega_A = 0.829$ and $(\omega_t^2 - \omega_0^2)^{1/2}/\Omega_A = 0.341$.

Note added in proof. We have now successfully completed calculations for the composite splay and bending solitons; their profiles, energies, and NMR frequencies. In particular, the composite splay soliton consists of the $\hat{l}$ vector in a splaylike configuration and the $\hat{d}$ vector in a bendlike configuration. Its NMR responses are $R_l = 0.635$, $R_t = 0.823$. Furthermore, the composite splay soliton has lower energy than the corresponding pure-$\hat{l}$ texture. We believe that it is the composite splay soliton that is responsible for the transverse satellite resonance in the Gould-Lee experiment. These and a proposal for an experiment to further test the soliton hypothesis will be published separately.[14]

APPENDIX: STABILITY OF TWIST *l* textures

Here we will study the stability of twist $\hat{l}$ texture against small oscillation in both $\hat{l}$ and $\hat{d}$ vectors. Assuming $\hat{d}$ and $\hat{l}$ are given by

$$\hat{d} = (1-g^2)^{1/2}((1-\psi^2)^{1/2}\hat{y} + \psi\hat{x}) + g\hat{z}\,,$$
$$\hat{l} = (1-\theta^2)^{1/2}(\cos\chi\hat{y} + \sin\chi\hat{x}) + \theta\hat{z}\,, \tag{A1}$$

where g, ψ, and θ are assumed to be small. Substituting this into Eq. (3) and subtracting the equilibrium value [i.e., $g = \psi = \theta = 0$, and $\chi = \chi_0(z) = 2\tan^{-1}\exp(2z/\xi)$] for pure twist structure we have

$$\frac{\delta f}{\sigma_3} = \tfrac{1}{2}A\left(-8\xi^{-2}\int_{-\infty}^{\infty} dz\,\tanh\frac{2z}{\xi}\,\mathrm{sech}\frac{2z}{\xi}\,\psi(z) + \int_{-\infty}^{\infty} dz\{\chi_z'^2 + 4\psi_z^2 + 4\xi^{-2}[1-2\cos^2\chi_0(z)](\chi'-\psi)^2 + \theta_z^2 + 4g_z^2 + 4\xi^{-2}[\cos^2\chi_0(z)\,\theta^2 + g^2 - 2\cos\chi_0(z)\theta g]\}\right), \tag{A2}$$

where $\chi' = \chi - \chi_0(z)$.

We note that the fluctuations are separable into two modes $[(\chi',\psi)$ and $(\theta,g)]$. (χ',ψ) mode can be further simplified by introducing new variables by

$$u = \chi + 4\psi \quad \text{and} \quad v = \chi - \psi\,. \tag{A3}$$

Then the quadratic terms in χ', ψ are transformed as

$$\delta f(\chi',\psi) = \tfrac{1}{2}A\int_{-\infty}^{\infty} dz\left[\tfrac{1}{5}u_z^2 + \tfrac{4}{5}v_z^2 + 4\xi^{-2}\left(1 - 2\,\mathrm{sech}^2\frac{2z}{\xi}\right)v^2\right]. \tag{A4}$$

Then the eigenvalue equation for v

$$\lambda_v v = -\tfrac{4}{5}v_{zz} + 4\xi^{-2}[1 - 2\,\mathrm{sech}^2(2z/\xi)v] \tag{A5}$$

is easily solved as

$$\lambda_v = [\tfrac{1}{5}(2\sqrt{11} - 7)](4\xi^{-2}) \cong -0.077(4\xi^{-2})\,,$$

with

$$v \propto [\mathrm{sech}(2z/\xi)]^{(\sqrt{11}-1)/2}\,. \tag{A6}$$

The oscillation in v has a negative eigenvalue, which indicates that pure-$\hat{l}$ twist texture is unstable towards the formation of the composite soliton at least in the absence of current.

*Work supported by the NSF under Grant No. DMR76-21032.

[1]Spin $S=1$ state is a superposition of linear spin moment along two axis perpendicular to $\vec{S}$, like $l=1$ in the orbital case. The spin description of the A phase requires only one linear momentum direction $\hat{d}$. The A_1 phase on the other hand is a linear combination of two such vectors $\hat{d}_1$ and $i\hat{d}_2$.

[2]A. J. Leggett, Rev. Mod. Phys. 47, 331 (1976).

[3]Textures were first postulated and studied by de Gennes and co-workers; P. G. de Gennes, in *Proceedings of the Twenty-Fourth Nobel Symposium*, edited by B. Lundquist and S. Lundquist (Academic, New York, 1973), p. 112; also see P. G. de Gennes and D. Rainer, Phys. Lett. A 46, 429 (1974); and A. L. Fetter, Phys. Rev. B 14, 2801 (1976).

[4]N. D. Mermin and T. L. Ho, Phys. Rev. Lett. 35, 594 (1976).

[5]C.-R. Hu, P. Kumar and K. Maki (unpublished).

[6]K. Maki and T. Tsuneto, Phys. Rev. B 11, 2539 (1975); and K. Maki and H. Ebisawa, J. Low Temp. Phys. 23, 351 (1976).

[7]K. Maki and P. Kumar, Phys. Rev. B 14, 118 (1976); 14, 3920 (1976).
[8]K. Maki and P. Kumar, Phys. Rev. Lett. 38, 557 (1977); Phys. Rev. B 16, 182 (1977).
[9]O. Avenel *et al.*, in *Proceeding of Fourteenth International Conference on Low Temperature Physics*, Otaniemi, Finland, 1975, edited by M. Krusius and M. Vuorio (North-Holland, Amsterdam, 1975), Vol. 5, p. 429.
[10]C. M. Gould and D. M. Lee, Phys. Rev. Lett. 37, 1223 (1976).
[11]P. G. de Gennes, *Physics of Liquid Crystals* (Oxford University, London, 1974).
[12]V. Ambegaokar, P. G. de Gennes, and D. Rainer, Phys. Rev. A 9, 2676 (1974).
[13]J. Wheatley, Phys. Rev. 165, 304 (1968).
[14]K. Maki and P. Kumar (unpublished).